Surface reaction of bis(tertbutylimido)bis(diethylamido)tungsten precursor on Si(100) – (2×1)

Jin-Bao Wu, Yaw-wen Yang, Yi-Feng Lin, and Hsin-Tien Chiu

Citation: Journal of Vacuum Science & Technology A **21**, 1620 (2003); doi: 10.1116/1.1593050
View online: http://dx.doi.org/10.1116/1.1593050
View Table of Contents: http://scitation.aip.org/content/avs/journal/jvsta/21/5?ver=pdfcov
Published by the AVS: Science & Technology of Materials, Interfaces, and Processing

Surface reaction of bis(tertbutylimido)bis(diethylamido)tungsten precursor on Si(100)–(2×1)

Jin-Bao Wu
Department of Applied Chemistry, National Chiao Tung University, Hsinchu, Taiwan 30050, Republic of China

Yaw-wen Yang[a)]
Synchrotron Radiation Research Center, Hsinchu, Taiwan, 30077, Republic of China

Yi-Feng Lin and Hsin-Tien Chiu[b)]
Department of Applied Chemistry, National Chiao Tung University, Hsinchu, Taiwan 30050, Republic of China

(Received 19 November 2002; accepted 12 May 2003; published 16 July 2003)

Thermal decomposition of a metal-organic chemical vapor deposition precursor, $(t\text{-BuN}{=})_2\text{W}(-\text{NEt}_2)_2$, (bis(tertbutylimido)bis(diethylamido)tungsten, on Si(100) has been studied by means of synchrotron radiation-based x-ray photoemission spectroscopy and temperature programmed desorption spectroscopy. The resultant thin films consist of tungsten metal, silicon carbides and silicon nitrides. Major desorption products originated from ligand decomposition include imine ($C_2H_5N{=}CHCH_3$) that is derived from β-H elimination of diethylamido ligand, and isobutene (C_4H_8) that is generated from γ-H elimination of *t*-butylimido ligands. The transmetalation of the precursor leads to tungsten metal adsorption on Si(100); by contrast, tungsten nitrides, tungsten carbides and tungsten oxides are produced as the same precursor is decomposed on SiO_2 surface. © *2003 American Vacuum Society.* [DOI: 10.1116/1.1593050]

I. INTRODUCTION

Chemical vapor deposition (CVD) is an important technique that has found wide utilization in modern industry to produce a broad range of materials.[1,2] Perhaps, one of the most notable examples is the successful synthesis of diamond films. The basic process involves a thermal decomposition of gaseous precursors on a heated substrate to produce thin films of desired properties and all the ligands of the precursors should be completely removed as volatile species. However, an incomplete ligand removal can result in the contamination of the films. Therefore, an understanding of how the precursor undergoes thermolysis in terms of elementary processes can be extremely useful in refining the molecular design of the precursors and achieving a low impurity incorporation in the films.[3–5]

Metal nitrides are of particular interest in microelectronic device fabrication because of the unusual properties associated with nitride materials such as high mechanical hardness, high thermal and chemical stability. Continuous shrinking of the feature dimension in ultralarge-scale-integrated circuits mandates a transition from aluminum to copper metallization scheme to keep pace with the device performance enhancement. However, copper is highly mobile in Si and also reactive with Si and SiO_2. A utilization of copper interconnect technology necessitates the deployment of barrier materials that effectively retard Cu diffusion into underneath structures. In this aspect, nitrides of heavier refractory metals like tantalum[6] and tungsten[7–9] have shown great promise as robust barrier materials.

We have been particularly interested in designing metal nitride precursors and achieving a CVD deposition of metal nitride films. The synthesis strategy consists of joining amido (–NR, R=alkyl group) and/or imido (=NR) ligands to the metal center.[10] The double bond of the imido ligand is expected to survive the thermolysis better owing to its higher bond strength than the single bond of amido ligand. The CVD deposition of metal nitride films was typically carried out in a cold-wall reactor.[11,12] Along this line of molecular designing of the CVD precursor, Bchir *et al.* recently demonstrated the applicability of tungsten imido complex in producing effective barrier films.[13] In the present article, we report on an *in situ* surface science study aimed to illuminate the thermal decomposition of the precursor in its early stage using high energy resolution, synchrotron radiation based x-ray photoelectron spectroscopy (SR-XPS) and temperature programmed desorption spectroscopy (TPD) to characterize both the thin films and gaseous desorption products during the thermolysis on Si(100) surface.

II. EXPERIMENT

Experiments were performed in a mu-metal spherical chamber with a chamber base pressure of better than 3×10^{-10} Torr. Major instruments installed in the chamber included a differentially pumped quadrupole mass spectrometer (UTI 100 C) for TPD, a low energy electron diffraction apparatus, a differentially pumped sputter ion gun, and a triple-channeltron VG electron energy analyzer.[14]

Photoemission measurements were carried out at the wide range spherical grating monochromator beamline of Syn-

[a)]Author to whom correspondence should be addressed; electronic mail: yang@srrc.gov.tw
[b)]Electronic mail: htchiu@cc.nctu.edu.tw

chrotron Radiation Research Center. This beamline is equipped with a set of six spherical gratings to deliver soft x-ray photons with energy ranging from 15 to 1500 eV. All the reported XPS spectra were first normalized to photon flux by dividing recorded XPS signal by photocurrent derived from a gold mesh situated in the beamline. Binding energy scale was referenced to bulk Si $2p_{3/2}$ core level at a binding energy of 99.2 eV relative to Fermi level in order to facilitate comparisons with the published binding energies for the other elements. For measurements at cryogenic temperature, owing to surface photovoltage effect, a rigid shift of Si $2p$ core level toward higher binding energy by ~0.6 eV had to be corrected for *n*-type sample used here.[15]

Two different methods for mounting the Si(100) sample (*n*-type $\rho=1-10\ \Omega\,\mathrm{cm}$) were used here. For the photoemission measurements, a scheme similar to that reported earlier was used because of its heating uniformity across the sample.[16] For TPD measurements, the Si sample was mounted differently to ensure a linear temperature ramping that could be quite difficult to achieve otherwise due to a precipitous resistivity drop across ~450 K as thermal excitation of carrier became pronounced. In our arrangement, a flat Ta sheet (0.025 mm thick) was sandwiched tightly between two Si samples, and together they were held by two Ta clips. Initial resistive heating was achieved by passing current through the Ta sheet until at higher temperatures, as the Si sample became more conductive than the Ta sheet, a direct heating of Si sample then became possible. The linearity of sample heating was quite satisfactory and the working temperatures could be varied between 100 and 1400 K. Moreover, the readings from thermocouples were further calibrated against published H_2 desorption temperature data.[17]

The cleaning of Si(100) was done by sputtering and annealing. A thin SiO_2 film was grown by bombarding Si(100) kept at 900 K with 400 eV oxygen ions generated from backfilling a sputter ion gun with O_2. The Si $2p$ XPS spectrum was monitored until it reached a steady state and a typical oxide formation time lasted about 2 h. The metal-organic CVD (MOCVD) precursor, $(t\text{-BuN}{=})_2\mathrm{W}(-\mathrm{NEt}_2)_2$, (bis-(tertbutylimido)bis(diethylamido)tungsten (BTBDT) was synthesized based on a published procedure.[10] Results for another precursor, $(t\text{-BuN}{=})_2\mathrm{W}(-\mathrm{NHBu}\text{-}t)_2$, bis(tertbutylimido)bis(tertbutylamido)tungsten (BTBTT), are occasionally cited for comparison. These two precursors are isomers, but the former has two hydrogen atoms at the β site while the latter has none. Note the α site is counted from the N end of the ligand.

Dosing was done with a glass doser terminated with a 0.5 mm pinhole. A gas manifold was constructed from glass as much as possible to minimize the potential precursor decomposition on metallic parts during the transfer to the sample. Immediately prior to the dosing, the headspace in the precursor reservoir was evacuated again to remove any volatile ligand species that might have accumulated owing to the decomposition of the precursor. Even with all these precautions, a successful adsorption of the intact precursor, evidenced by the emergence of W-containing desorption peaks like 284 amu, does not commence until a full passivation of the transfer line is reached.

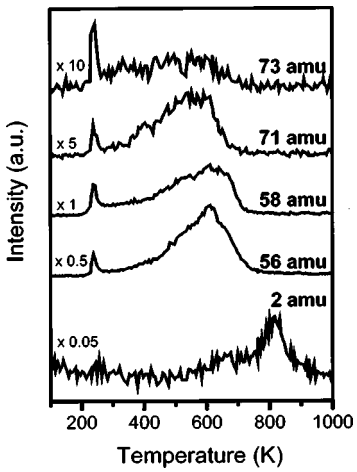

FIG. 1. Multimass TPD spectra for slightly more than 1 monolayer of BT-BDT initially adsorbed on Si(100) at 100 K. The heating rate was about 3 K/s.

III. RESULTS AND DISCUSSION

Figure 1 shows multimass thermal desorption spectra obtained for BTBDT decomposed at higher temperature on Si(100). Surface coverage is slightly more than one completed chemisorbed layer and the common desorption peaks found for all hydrocarbons at 240 K are attributed to the cracking fragments of the physisorbed BTBDT. Both *t*-butylamine and diethylamine have identical molecular weight of 73 amu, but the largest cracking fragment detected for *t*-butylamine is only 58 amu so the 73 amu species is entirely due to diethylamine. The intense 71 amu desorption peak is assigned to imine, $\mathrm{C_2H_5N{=}CHCH_3}$, formed via a β-H elimination accompanied by the W–N bond cleavage. This imine species is derived from the diethylamido, not *t*-butylimido, ligand. The desorption of both 73 and 71 species starts right after physisorption state until their completion at about 670 K.

Next, the appearance of 58 amu species, predominately derived from *t*-butylamine, signifies a recombinative desorption of the *t*-butylimido ligand with surface hydrogen. The 56 amu mass, isobutene $\mathrm{C_4H_8}$, is another abundant species that is derived from the decomposition of the *t*-butylimido ligand. The occurrence of H elimination at the γ site and the bond scission between N and β-C accounts for the formation of isobutene. This reaction scheme is in accord with the finding of isobutene from pentane radical desorption on Ni(100).[18] The desorption of isobutene and *t*-butylamine accounts for the major decomposition pathway of *t*-butylimido ligand. It is noted that the desorption temperatures for 58 amu are some 50° higher than those for 73 and 71, perhaps attributable to stronger M=N bond in imido than that in amido ligands. Other small hydrocarbons can also be detected but their identification tends to be plagued by the presence of cracking fragments from higher masses. Hence these species are omitted here. Finally, hydrogen atoms, formed almost

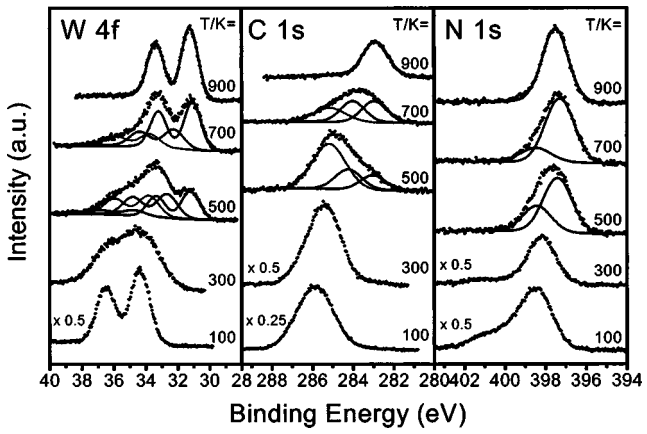

FIG. 2. Change of W $4f$, C $1s$, and N $1s$ SR-XPS spectra with the annealing temperature for ~1.5 ML of BTBDT precursor adsorbed on Si(100). Selective presentation of the least-squares fitting results is shown to illustrate the evolution of main components. X-ray energy is fixed at 600 eV.

exclusively from C–H bond scission during the decomposition, are retained on Si(100) surface until a much higher temperature is reached. The major desorption peak at 810 K and the minor one at 650 K represent the desorption from monohydride and dihydride phases, respectively.[17]

Figure 2 presents the change of W $4f$, C $1s$, and N $1s$ SR-XPS spectra with the annealing temperature for ~1.5 monolayer of BTBDT initially dosed on Si(100) at 100 K. The annealing was done at a 100 K temperature increment, but for clarity only the alternate spectra are presented. The sharp W $4f$ peak seen at 100 K with W $4f_{7/2}$ core level at 34.4 eV is assigned to molecular-intact BTBDT. A warmup to 300 K leads to a considerable broadening of W $4f$, suggesting the formation of multiple products due to the incomplete ligand removal. After annealing to 500 K, the broadened peak shifts to lower binding energy and the formation of a new peak with its W $4f_{7/2}$ at 31.2 eV is observed. This peak is due to W metal and its value agrees closely with 31.3 eV value from the Handbook.[19] A further annealing to 700 K sees a continuous increase of W metal peak at the expense of other W component. After annealing to 900 K, the transformation to W metal is complete and the binding energy of W $4f_{7/2}$ peak is right at 31.3 eV.

The peak fitting was carried out based on a nonlinear least squares algorithm. An integral Shirley background in conjunction with line shape functions generated from the products between Gaussian and Lorentzian functions are found to be adequate for describing the acquired spectra. In a given spectrum, the Gaussian with (Γ_G) and the Lorentzian width (Γ_L) are allowed to vary in the fits but constrained to be the same for all peaks. Moreover, the spin orbit splitting and branching ratio in the W doublet is fixed at 2.18 eV and 0.75, respectively. The XPS fit also shows that the W metal spectrum can be described by a single component with a width of 1.2 eV. The emergence of metallic W peak at 500 K indicates that some of surface-adsorbed BTBDT precursor molecules already decompose completely. The shift of W $4f$ peak toward lower binding energy at higher temperature is consistent with the oxidation state decrease of the W atom after the ligand loss. Both amido and imido ligands are expected to exhibit electron-withdrawing character because the nitrogen atom in the ligand has highest electronegativity.

It is noted that the temperature at which the metallic W begins to emerge depends on initial coverage and the type of precursor in use. At submonolayer coverage, the formation temperature of metallic W can drop to about 300 K, indicating the reactive nature of Si(100) surface. The same phenomenon of a complete ligand transfer from the precursors to metal substrate has been reported in previous surface reaction studies of hexafluoroacetylacetonato complexes of transition metals like Rh,[20] Pd,[21] and Pt[20] deposited on Cu(111) as well as metal complexes of Pd and Pt deposited on supports.[22] The present results show that this type of so-called redox transmetalation reaction, metal atoms transferred from the precursor to the substrate while being reduced, can be observed on semiconductor surface as well.

The C $1s$ peak first appears at 285.9 eV and it has a relatively large width of 2.0 eV, consistent with the presence of a small amount of coadsorbed amines generated through the reaction of the precursor with the metallic surface in the gas manifold. After a 500 K annealing, a low binding energy peak at 282.9 eV appears and this peak continues to gain in intensity but its energy position remains the same for higher annealing temperatures. The peak at 282.9 eV is in line with the reported binding energy values for the Si carbides: 282.5,[23] 283.4,[23] and 283.6 eV.[24] The justification for forming Si carbides, instead of WC, is grounded on the finding of zero-valent state for W in the films.

The binding energy for the N $1s$ peak at 100 K is 398.5 eV and the small peak at 401.1 eV is assigned to the coadsorbed amine molecules that form molecular-intact dative bonding with the down atoms of the silicon dimers in the reconstructed Si surface.[25–27] The dative bonding is replaced by the normal dissociative chemisorption bonding of the amine at 300 K. Annealing to 500 K shifts the whole N $1s$ peak to lower binding energy and the peak fitting resolves a lower binding energy peak at 397.5 eV. After 900 K annealing, this peak narrows down to a width of 1.4 eV and its binding energy value is the same as that of Si nitride at 397.5 eV.[19] Again, the basis for Si nitride assignment comes from the zero-valent state for W in the films because the binding energy difference between WN_x and Si nitride is rather small (<0.5 eV).

There are only minor changes for Si $2p$ spectra after annealing. The main reason is that the Si $2p$ spectrum taken with 600 eV photons is dominated by the bulk Si $2p$ component and the surface-sensitive feature like the small peak attributed to the downatom of the dimer is not distinct at all. As a result, the Si $2p$ peak serves more like an energy reference in the present experiments that can be used to minimize the energy uncertainty from band bending.

The change of W $4f$, C $1s$, and N $1s$ signal with annealing temperature is highlighted in Fig. 3. The data in Fig. 3 are obtained by integrating the respective core level spectra

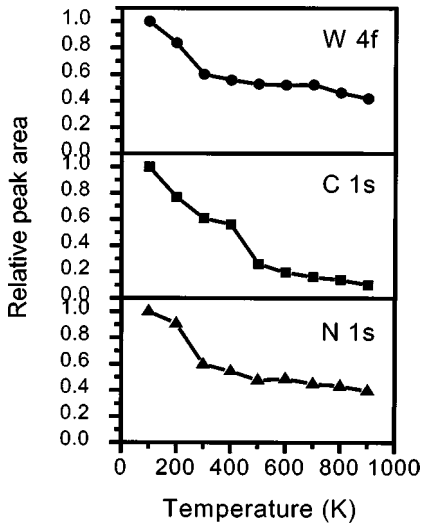

FIG. 3. Temperature dependence of the normalized integrated areas of W 4*f*, C 1*s*, and N 1*s* peaks using the data reported in Fig. 2. The normalization is done by setting the respective peak area at 100 K as one unit.

presented in Fig. 2. The drastic change of peak area between 100 and 300 K results from a combined effect of morphology change of the BTBDT film during the warmup and the desorption of physisorbed BTBDT at about 240 K. The W 4*f* signal remains pretty much the same throughout annealing temperature, indicating the insignificant desorption of W-containing species. After 900 K annealing, the C 1*s* signal decreases to 1/6 of its value at 300 K. The dramatic change seen between 300 and 600 K is consistent with the intense desorption of isobutene and *t*-butylamine. It is noted that the temperature scale read from Fig. 3 deviates from that in Fig. 1 because of the variation of the way the surface was heated in two measurements. For N 1*s* signal after 900 K annealing, the signal decreases to 2/3 of its value at 300 K, suggesting the retention of N atoms by Si surface once the amine ligands break off from the precursor. Based on the combined TPD and XPS results, the surface reaction pathways assumed by the BTBDT precursor on Si(100) at elevated temperatures are presented in Fig. 4.

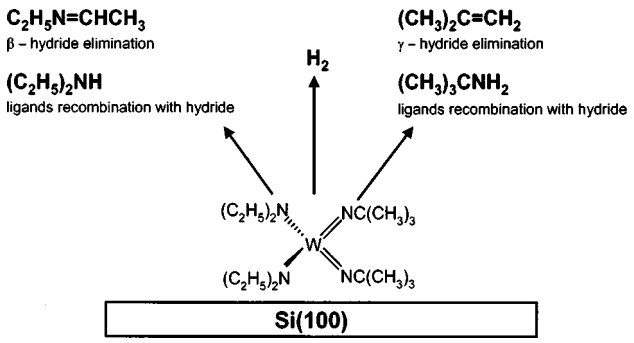

FIG. 4. Surface reaction pathway of BTBDT on Si(100). Major decomposition pathways are γ-H elimination in *t*-butylamine ligand side to form isobutylene, and β-H elimination in diethylamine ligand side to produce the imine species, respectively. The eventual formation of W metal and silicon nitrides and silicon carbides are observed after 900 K.

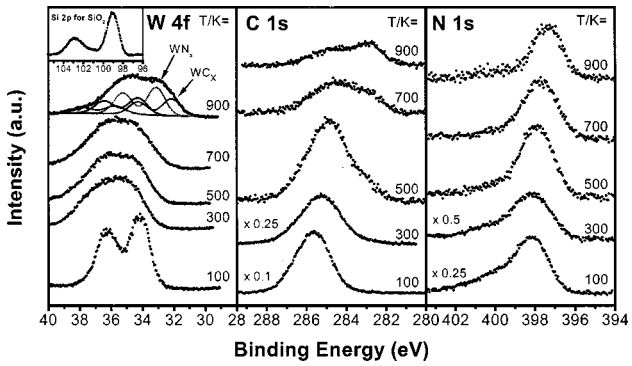

FIG. 5. Change of W 4*f*, C 1*s*, and N 1*s* SR-XPS spectra with the annealing temperature for BTBDT adsorbed on SiO_2 with its Si 2*p* spectrum shown in the inset. The dosage was the same as that used in Fig. 2. Again, the energy of the x ray is fixed at 600 eV.

The finding of W metal after the precursor decomposition is astonishing because, first, a transfer of the tungsten metal atom from the precursor to Si(100), i.e., transmetalation, requires simultaneous breakings of two W═N double bonds and two W–N single bonds, which is energetically costly. Second, in the previous CVD deposition using both BTBDT and BTBTT precursors, WN_x products are formed exclusively, as evidenced by the data from x-ray diffraction, XPS, etc.[12] Why is there a difference in end products? Can WN_x be formed under ultrahigh vacuum conditions? The CVD reaction was carried out in a hot-wall reactor and the originally clean Si surface was replaced by a steady-state surface covered with all sorts of product species including nitrides and carbides. The ''real'' substrate in CVD reaction is exceedingly complex and thus difficult to model after. Instead, we performed another precursor-decomposition experiment on a clean SiO_2 surface conveniently prepared according to the method described earlier.

Figure 5 shows the change of XPS spectra with the annealing temperature for BTBDT adsorbed on as-prepared clean SiO_2 surface. The BTBDT dosage is similar to that used in Fig. 2. The Si 2*p* XPS spectrum for the SiO_2 taken at the photon energy of 600 eV is also presented in the inset. The oxides exist predominately as the dioxide, evidenced by its Si 2*p* core level at 103.0 eV. The elemental Si 2*p* peak at 99.2 eV is attributed to the bulk, unreacted Si and shows a considerable broadening, presumably due to the structural damage incurred by oxygen ions. However, the most important consequence derived from the oxidation is that the reactive clean silicon surface atoms have been passivated through forming oxides. After annealing to higher temperatures, the Si 2*p* spectra for SiO_2 (data not shown) remain pretty much the same both in terms of peak width and peak shape except for a small decrease of intensity. This result suggests that given the present, relatively small BTBDT coverage, the Si atoms of SiO_2 fail to react with BTBDT to a large degree.

For the BTBDT precursor decomposition on SiO_2, the evolution of W 4*f* spectra with annealing temperature is completely different from what is observed on Si(100) and,

specifically, the W metal with its W $4f_{7/2}$ at a binding energy of 31.3 eV does not appear throughout the annealing. Moreover, a gradual sharpening of W $4f$ core levels with the annealing temperatures never occurs, which is equivalent to say that a detachment of amido and imido ligands from W metal center never occurs to a completion. The peak fitting with the characteristic feature of component peaks constrained to be the same results in four W $4f_{7/2}$ components: 32.2, 33.2, 34.3, and 35.7 eV. It should be mentioned that the peak fitting alone does not provide a single solution. Nevertheless, the qualitative picture such as the lack of W metal and the presence of W compounds with W in high oxidation state should be valid, thanks to the favorable location of these peaks at both ends of the spectrum. The 32.2 and 33.2 eV components are assigned to WC_x,[19] WN_x,[12] respectively. The latter two components are attributed to W oxides of varying oxygen content and, by comparison, the listed W $4f_{7/2}$ binding energies for WO_2 and WO_3 are 32.8 and 35.8 eV, respectively.[19] Apparently, the reaction between BTBDT and the SiO_2 does takes place and produces W oxides. At annealing temperature higher than 500 K, there is already an increasing spectra weight at about 36 eV, a region where oxide peaks lie. This oxidation reaction is mainly driven by a large enthalpy change derived from the large enthalpies of formation of W oxides.[28]

Turning to C $1s$ spectra, it is apparent that different C species are formed and two broad peaks can be identified in the 900 K annealed spectrum with their C $1s$ binding energies at 282.4 and 284.6 eV. The former is assigned to WC peak despite its value being 0.4 eV smaller than that listed in the Handbook,[19] whereas the latter one is due to graphitic carbons. As for the N $1s$ spectra, the annealing to 900 K produces a peak at 397.4 eV, attributed to WN_x and its width of 1.8 eV is larger than the corresponding one of 1.4 eV in Fig. 2.

The products formed between BTBDT on Si(100) and BTBDT on SiO_2 are very different. We speculate on the following reasons. The SiO_2 is an insulating oxide and is rather inert; consequently, the electronic property of the surface should be less important in catalyzing the surface reaction.[29] For instance, alkylsilanes are found to decompose thermally on Si(100) into a series of products at elevated temperatures, whereas no adsorption of alkylsilanes on SiO_2 can even be observed.[30] The decomposition reaction on this kind of surface could be more like a thermolysis, with no clear preference given to any particular bonds. In other words, bond breaking is weighed according to the relative strength in C–C, C–H, and N–C bonds. As a result, the broad product distribution found on SiO_2 seems to be a manifest of this nonselective bond breaking process. In stark contrast, the preferential cleavage at the W–N bond found on Si(100) underlines the importance of surface electronic property.

In brief summary, our results demonstrate that, for a large MOCVD precursor such as BTBDT with 59 atoms per molecule, selective bond breaking activated by reactive surface like Si(100) can take place. In the example presented here, all the ligands bonded to the W metal center are stripped away in a so-called transmetalation process to produce W metal, silicon nitrides, and silicon carbides. In comparison, the same BTBDT decomposition on the SiO_2 produces WN_x and graphitic carbons.

ACKNOWLEDGMENTS

Y.W.Y. thanks SRRC for in-house equipment grant and National Science Council of R.O.C. for Grant No. NSC 90-2113-M-213-015. H.T.C. is grateful for the support from NSC through Grant No. NSC-90-2113-M-009-022.

Presented at the 49th International Symposium of AVS, Denver, CO, 4–8 November 2002.

[1]W. S. Rees, *CVD of Nonmetals* (VCH, Weinheim, 1996).
[2]T. Kodas and M. Hampden-Smith, *The Chemistry of Metal CVD* (VCH, Weinheim, 1994).
[3]C. M. Truong, P. J. Chen, J. S. Corneille, W. S. Oh, and D. W. Goodman, J. Phys. Chem. **99**, 8831 (1995).
[4]G. Ruhl, R. Rehmet, M. Knizová, R. Merica, and S. Veprek, Chem. Mater. **8**, 2712 (1996).
[5]J. Cheon, L. H. Dubois, and G. S. Girolami, J. Am. Chem. Soc. **119**, 6814 (1997).
[6]M. Takeyama, A. Noya, T. Sase, A. Ohta, and K. Sasaki, J. Vac. Sci. Technol. B **14**, 674 (1996).
[7]R. R. Ivanova, C. J. Galewski, C. A. Sans, T. E. Seidel, S. Grunow, K. Kumar, and A. E. Kaloyeros, Mater. Res. Soc. Symp. Proc. **564**, 321 (1999).
[8]M. Uekubo, T. Oku, K. Nii, M. Murakami, K. Takahiro, S. Yamaguchi, T. Nakano, and T. Ohta, Thin Solid Films **286**, 170 (1996).
[9]J. E. Kelsey, C. Goldberg, G. Nuesca, G. Peterson, A. E. Kaloyeros, and B. Arkles, J. Vac. Sci. Technol. B **17**, 1101 (1999).
[10]H.-T. Chiu, S.-H. Chuang, C.-E. Tsai, G.-H. Lee, and S.-M. Peng, Polyhedron **17**, 2187 (1998).
[11]M. H. Tsai, S. C. Sun, H. T. Chiu, and S. H. Chuang, Appl. Phys. Lett. **68**, 1412 (1996).
[12]H. T. Chiu and S. H. Chuang, J. Mater. Res. **8**, 1353 (1993).
[13]O. J. Bchir, S. W. Johnston, A. C. Cuadra, T. J. Anderson, C. G. Ortiz, B. C. Brooks, D. H. Powell, and L. McElwee-White, J. Cryst. Growth **249**, 262 (2003).
[14]Y. W. Yang and L. J. Fan, Langmuir **18**, 1157 (2002).
[15]E. Landemark, C. J. Karlsson, Y. C. Chao, and R. I. G. Uhrberg, Phys. Rev. Lett. **69**, 1588 (1992).
[16]H. Nishino, W. Yang, Z. Dohnálek, V. A. Ukranitsev, W. J. Choyke, and J. T. J. Yates, J. Vac. Sci. Technol. A **15**, 182 (1997).
[17]K. Sinniah, M. G. Sherman, L. B. Lewis, W. H. Weinberg, J. T. J. Yates, and K. C. Janda, J. Chem. Phys. **92**, 5700 (1990).
[18]F. Zaera and S. Tjandra, J. Am. Chem. Soc. **118**, 12738 (1996).
[19]J. F. Moulder, W. F. Stickle, P. E. Sobol, and K. D. Bomben, in *Handbook of X-ray Photoelectron Spectroscopy*, edited by J. Chastain (Perkin-Elmer Corp., Eden Prairie, MN, 1992).
[20]E. L. Crane, Y. You, R. G. Nuzzo, and G. S. Girolami, J. Am. Chem. Soc. **122**, 3422 (2000).
[21]W. Lin, R. G. Nuzzo, and G. S. Girolami, J. Am. Chem. Soc. **118**, 5988 (1996).
[22]J.-C. Hierso, R. Feurer, and P. Kalck, Chem. Mater. **12**, 390 (2000).
[23]K. L. Smith and K. M. Black, J. Vac. Sci. Technol. A **2**, 744 (1984).
[24]L. Muehlhoff, W. J. Choyke, M. J. Bozack, and J. T. J. Yates, J. Appl. Phys. **60**, 2842 (1986).
[25]S. F. Bent, J. Phys. Chem. B **106**, 2830 (2002).
[26]X. Cao and R. J. Hamers, J. Am. Chem. Soc. **123**, 10988 (2001).
[27]C. Mui, G. T. Wang, S. F. Bent, and C. B. Musgrave, J. Chem. Phys. **114**, 10170 (2001).
[28]J. A. Dean, *Lange's Handbook of Chemistry* (McGraw-Hill, New York, 1992).
[29]R. I. Masel, *Principles of Adsorption and Reaction on Solid Surfaces* (Wiley, New York, 1996), p. 769.
[30]M. Foster, B. Darlington, J. Scharff, and A. Campion, Surf. Sci. **375**, 35 (1997).